Conclusion

Thermal ion-molecule association reactions may be treated via RRKM theory[5,6,15] and thus also by the simplified computational schemes of Troe and co-workers[7,8] if neutral-neutral collision frequencies are replaced by ion-neutral frequencies (Langevin and ADO). Crucial inputs are the thermodynamic parameters of the association complex, especially the entropy.

Acknowledgment. This work was supported by Contract NAS7-100 (JPL Subcontract 954815) with the National Aeronautics and Space Administration.

Appendix I. List of Formulas

(a) ADO collision frequencies

$$Z_{ADO} = \frac{2\pi q}{\mu^{1/2}}\left[\alpha^{1/2} + C\mu_0\left(\frac{2}{\pi kT}\right)^{1/2}\right] \quad (A1)$$

where q is the charge of the ion, μ is reduced mass between colliders, α is polarizability of the molecule, μ_0 is the dipole moment of the molecule, C is the correction factor as derived in ref 2, and k is the Boltzmann constant.

(b) Harmonic oscillator density of states

$$\rho_{vib,h} = [E + a(E)E_Z]^{s-1}/(s-1)!\prod_{i=1}^{s}(h\nu_i) \quad (A2)$$

where E is the energy, E_Z is $^1/_2\sum_{i=1}^{s}h\nu_i$, s is number of oscillators, $a(E)$ is the empirical Whitten-Rabinovitch corrector, and ν_i are the vibrational frequencies.

(c) Anharmonicity correction factor

$$F_{anh} = \left(\frac{s-1}{s-3/2}\right)^m \quad (A3)$$

where m is the number of oscillators that disappear during the dissociation reaction.

(d) Energy dependence of the density of states corrector is given as

$$F_E \simeq \sum_{v=0}^{s-1}\frac{(s-1)!}{(s-1-v)!}\left(\frac{kT}{E_0 + a(E_0)E_Z}\right)^v \quad (A4)$$

(e) Rotational contribution

$$F_{rot} = [(s-1)!/(s+1/2)!]\{[E_0 + a(E_0)E_Z/kT]\}^{3/2} \times \left\{\frac{2.15(E_0/kT)}{2.15(E_0/kT)^{1/3} - 1 + [E_0 + a(E_0)E_Z/(s+1/2)kT]}\right\} \quad (A5)$$

(f) Internal rotation factor

$$F_{int\,rot} = \frac{(s-1)!}{(s-1/2)!}\left(\frac{E_0 + aE_Z}{kT}\right)^{1/2}\left[1 - \exp\left(\frac{-E_0}{sV_0}\right)\right]\left\{\left[1 - \exp\left(\frac{-kT}{V_0}\right)\right]^{1.2} + \frac{\exp(-1.2kT/V_0)}{\sqrt{2\pi I_m kT/\hbar^2}[1 - \exp(-\sqrt{n^2\hbar^2V_0/2I_m(kT)^2})]}\right\}^{-1} \quad (A6)$$

(20) R. C. Bolden and N. D. Twiddy, *Discuss. Faraday Soc.*, **53**, 192 (1972).
(21) D. B. Dunkin, F. C. Fehsenfeld, A. L. Schmeltekopf, and E. E. Ferguson, *J. Chem. Phys.*, **54**, 3817 (1971).
(22) N. G. Adams, D. K. Bohme, D. B. Dunkin, F. C. Fehsenfeld, and E. E. Ferguson, *J. Chem. Phys.*, **52**, 3133 (1970).
(23) (a) J. D. Poyzant, A. J. Cunningham, and P. Kebarle, *J. Chem. Phys.*, **59**, 5615 (1973); (b) D. A. Durden, P. Kebarle, and A. Good, *ibid.*, **50**, 805 (1969); (c) A. Good, D. A. Durden, and P. Kebarle, *ibid.*, **52**, 222 (1970).
(24) C. J. Howard, V. M. Bierbaum, H. W. Rundle, and F. Kaufman, *J. Chem. Phys.*, **57**, **57**, 3491 (1972).
(25) F. C. Fehsenfeld, M. Moseman, and E. E. Ferguson, *J. Chem. Phys.*, **55**, 2115 (1971).
(26) V. G. Anicich and M. T. Bowers, *J. Am. Chem. Soc.*, **96**, 1279 (1974).
(27) G. S. Janik and D. C. Conway, *J. Phys. Chem.*, **71**, 823 (1967).

Protein Hydration from Water Oxygen-17 Magnetic Relaxation

Bertil Halle,*† Thomas Andersson,‡ Sture Forsén,‡ and Björn Lindman†

Contribution from Physical Chemistry 1 and Physical Chemistry 2, Chemical Center, S-220 07 Lund 7, Sweden. *Received January 29, 1980*

Abstract: Water oxygen-17 magnetic relaxation is shown to be a powerful technique for studying protein hydration. Longitudinal and transverse ^{17}O relaxation rates were measured at variable frequency (4–35 MHz), temperature, pH, and protein concentration in aqueous solutions of seven proteins. The data were analyzed in terms of a fast exchange two-state model with local anisotropy. A water ^{17}O quadrupole coupling constant of 6.67 MHz and an order parameter of 0.06 (from ^{17}O splittings in lyotropic liquid crystals) results in approximately two layers of hydration water having a reorientational rate less than 1 order of magnitude slower than that of bulk water. This rapid local motion has a small anisotropic component, which is averaged out by protein reorientation with a correlation time of the order of 10 ns. Due to electrostatic protein–protein interaction the protein reorientation is considerably slower than predicted by the Debye–Stokes–Einstein equation. Charged residues, particularly carboxylate, are more extensively hydrated than other residues, accounting for the variation in the extent of hydration between different proteins.

Introduction

Despite the multitude of experimental techniques that have been used to study protein hydration,[1-3] a consistent picture of the structural and dynamical details of the protein–water interaction has still not emerged. Thus, it is worthwhile to search for new techniques to study the interacting water molecules as directly as possible.

To determine whether water ^{17}O magnetic relaxation is such a method, we have measured longitudinal and transverse ^{17}O

† Physical Chemistry 1.
‡ Physical Chemistry 2.

(1) Kuntz, I. D., Jr.; Kauzmann, W. *Adv. Protein Chem.* **1974**, *28*, 239.
(2) Eagland, D. In "Water-A Comprehensive Treatise"; Franks, F., Ed.; Plenum Press: New York, 1975; Vol. 4, Chapter 5.
(3) Berendsen, H. J. C. In "Water-A Comprehensive Treatise"; Franks, F.; Ed.; Plenum Press: New York, 1975; Vol. 5, Chapter 6.

0002-7863/81/1503-500$01.00/0

relaxation rates over a decade of resonance frequencies in aqueous solutions of seven proteins. (^{17}O relaxation rates in protein solutions have been reported in four previous studies. In two[4-5] of these the ^{17}O data alone did not yield any quantitative conclusions, whereas the other two[76,77] are concerned with specific interactions between water and protein-bound metals.)

Compared to proton and deuteron magnetic relaxation, which have been used extensively in protein hydration studies,[4,6-11] ^{17}O relaxation has at least four important advantages: (i) the strong quadrupolar interaction leads to large relaxation effects, thus permitting studies at reasonably low protein concentrations; (ii) the intramolecular origin of the electric field gradient at the water oxygen nucleus makes the quadrupolar interaction virtually independent of the molecular environment, which greatly facilitates the interpretation of relaxation data; (iii) except for a narrow pH range around neutral, the ^{17}O relaxation is not influenced by proton (deuteron) exchange with prototropic residues on the protein, which is a serious problem in ^{1}H and ^{2}D relaxation,[12,37] but can only be affected by exchange of entire water molecules (the ^{17}O-exchange broadening around neutral pH may be eliminated through proton decoupling[13]); (iv) cross-relaxation, which contributes significantly to ^{1}H relaxation,[71] is unimportant for ^{17}O.

Experimental Section

Materials. Human plasma albumin (HPA) was obtained from AB KABI, Stockholm, as a freeze-dried preparation (batch no. 50412) and was used without further purification. HPA solutions were prepared by weight, assuming 95% purity.[59]

Horse heart cytochrome *c* (cyt *c*) was prepared by the method of Margoliash and Walasek[14] and further purified on an ion-exchange resin to separate deamidated forms from the native protein (the result was checked by gel electrophoresis). Reduced cyt *c* was prepared by ascorbate reduction and salt removed by dialysis. For the measurements on D_2O solutions, the protein was lyophilized and redissolved in D_2O.

Human (adult) oxyhemoglobin (Hb) was prepared by the ammonium sulfate method[15] and deionized on an ion-exchange column.

Parvalbumin (PA), p*I* = 4.25, from carp muscle (*Cyprinus carpio*) was isolated by the method of Pechère et al.[16] and stored as lyophilized powder.

Hen egg white lysozyme (Lyz), grade 1, was purchased from Sigma Chemical Co. as lyophilized powder and was used without further purification.

Horse liver alcohol dehydrogenase (ADH), apoenzyme with the two catalytic Zn^{2+} ions removed, was a gift from Dr. Inger Andersson. The protein was prepared by the method of Maret et al.[19]

Human (polyclonal) immunoglobulin G was a gift from Dr. C. Borrebaeck, Biochemistry 2, Chemical Center, Lund, Sweden.

Protein concentrations (except HPA) were determined spectrophotometrically by using $\epsilon^{550} = 29.5$ cm^{-1} mM^{-1} (ferro cyt *c*),[18] $a^{541} = 0.85$ cm^{-1} mg^{-1} mL (Hb),[15] $\epsilon^{259}-\epsilon^{269} = 1000$ cm^{-1} mM^{-1} (PA),[17] $a^{280} = 2.65$ cm^{-1} mg^{-1} mL (Lyz),[18] $a^{280} = 0.45$ cm^{-1} mg^{-1} mL (ADH),[19] $a^{280} = 1.32$ cm^{-1} mg^{-1} mL (IgG).[18]

All protein solutions were made from doubly distilled (quartz apparatus) water or 99.7 atom % D_2O (Ciba-Geigy) and used within 24 h of preparation. H_2O or D_2O enriched to 10 atom % in ^{17}O (Biogenzia Lemania, Lausanne) was added to obtain protein solutions with ca. 1 atom % ^{17}O. pH (pD) was adjusted with HCl and KOH (DCl and KOD). For the HPA solutions we used KCl (Suprapur, Merck).

pH measurements were made with a Radiometer PHM 52 instrument equipped with a GK 2322C combination electrode. For the potentiometric titration (HPA in D_2O) we used a thermostated titration vessel with nitrogen atmosphere and a microburette. Conversion to pD values was made according to[20] pD = pH* + 0.45, where pH* is the instrument reading for a D_2O solution with the electrode calibrated in standard H_2O buffers.

Relaxation Measurements. Oxygen-17 relaxation rates were measured at four frequencies: (i) at 34.565 MHz on a home-built Fourier-transform spectrometer equipped with a 6 T magnet (Oxford Instrument Co. Ltd.), (ii) at 13.564 MHz on a modified Varian XL-100-15 Fourier-transform spectrometer using an external proton lock, (iii) at 8.256 and 3.994 MHz on a Bruker BKr-322s spectrometer with a Varian V-71 computer using a home-made interface and program. Longitudinal relaxation rates were measured by inversion recovery (π-τ-$\pi/2$ pulse sequences). Transverse relaxation rates were obtained from the line width $\Delta\nu_{obsd}$ at half-height of the absorption curves according to $R_{2,obsd} = \pi\Delta\nu_{obsd}$, except at the two lowest frequencies where the Carr-Purcell-Meiboom-Gill sequence was employed. At least three separate measurements were made for each data point. The probe temperature was kept constant within 0.2 °C by passage of dry thermostated air or nitrogen. We used sample tubes with an outer diameter of 12 or 8 mm (Bruker). The nonlinear fits of the dispersion data were made with a modified Marquardt algorithm.[21]

Proton-Exchange Broadening. Around neutral pH the water proton exchange is sufficiently slow to produce a broadening of the ^{17}O absorption peak.[69] At 27 °C the pH dependence of the line width in H_2O is almost symmetrically peaked around pH 7.2, where the exchange broadening amounts to ca. 70 Hz. The ^{17}O dispersion data were obtained from protein solutions with pH at least 1.8 units from the maximum; the broadening is then less than 2 Hz and may be corrected with the help of pure H_2O data. Due to additional catalytic mechanisms for proton exchange in the presence of prototropic side chains, the real exchange broadening correction is always smaller than for pure H_2O. Data points around neutrality are therefore uncertain and have been omitted (Figure 7). The smaller magnetic moment of the deuteron (compared to the proton) results in a smaller exchange broadening in D_2O (12 Hz maximum at pD 7.6). This is the reason that some of the experiments reported here were done on D_2O solutions.

Results

Relaxation Theory. The relaxation theory for the oxygen-17 nucleus is complicated by the large spin quantum number $^5/_2$. If the molecular motion causing quadrupolar relaxation has components with correlation times of order of the inverse resonance frequency $1/\omega_0$ or longer, i.e., if in its spectral density $J(0) \neq J(\omega_0)$ (so-called "nonextreme narrowing" conditions), then the relaxation must be described by a sum of three decaying exponentials.[22,28]

If the ^{17}O nucleus exchanges between environments with different intrinsic relaxation rates, even more exponentials are needed to describe the decaying nuclear magnetization. For the important case of fast exchange, i.e., when the exchange rates exceed the intrinsic relaxation rates, the relaxation matrix **R** may be decomposed according to[23] eq 1, where the sum runs over all environments ("states") S and P_S is the fraction of nuclei in state S.

$$\mathbf{R} = \sum_S P_S \mathbf{R}_S \qquad (1)$$

For spin $^5/_2$ it is not possible to obtain general analytical expressions for the decay of the longitudinal and transverse magnetization, but numerical computations[24] for a two-state model

(4) Koenig, S. H.; Hallenga, K.; Shporer, M. *Proc. Natl. Acad. Sci. U.S.A* **1975**, *72*, 2667.
(5) Glasel, J. A. *Nature (London)* **1968**, *218*, 953.
(6) Hallenga, K.; Koenig, S. H. *Biochemistry* **1976**, *15*, 4255.
(7) Grösch, L.; Noack, F. *Biochim. Biophys. Acta* **1976**, *453*, 218.
(8) Gaggelli, E.; Tiezzi, E.; Valensin, G. *Chem. Phys. Lett.* **1979**, *63*, 155.
(9) Oakes, J. *J. Chem. Soc., Faraday Trans. 1* **1976**, *72*, 216.
(10) Eley, D. D.; Hey, M. J.; Ward, A. J. I. *J. Chem. Soc., Faraday Trans. 1* **1975**, *71*, 1106.
(11) Kuntz, I. D., Jr.; Brassfield, T. S.; Law, G. D.; Purcell, G. V. *Science (Washington, D.C.)* **1969**, *163*, 1329.
(12) Tait, M. J.; Franks, F. *Nature (London)* **1971**, *230*, 91.
(13) Earl, W. L.; Niederberger, W. *J. Magn. Reson.* **1977**, *27*, 351.
(14) Margoliash, E.; Walasek, O. F. *Methods Enzymol.* **1976**, *10*, 339.
(15) Antonini, E.; Brunori, M. "Hemoglobin and Myoglobin and Their Reactions with Ligands"; North Holland Publishing, Co.: Amsterdam, London, 1971; Chapter 1.
(16) Pechère, J.-F.; Demaille, J.; Capony, J.-P. *Biochim. Biophys. Acta* **1971**, *236*, 391.
(17) Parello, J., private communication.
(18) Sober, H. A.; Ed. "Handbook of Biochemistry", 2nd ed.; CRC Press: Cleveland, Ohio, 1970.
(19) Maret, W.; Andersson, I.; Deitrich, H.; Schneider-Bernlöhr, H.; Einarsson, R.; Zeppezauer, M. *Eur. J. Biochem.* **1979**, *98*, 501.
(20) Covington, A. K.; Paabo, M.; Robinson, R. A.; Bates, R. G. *Anal. Chem.* **1968**, *40*, 700.
(21) Bevington, P. R. "Data Reduction and Error Analysis for the Physical Sciences"; McGraw-Hill: New York, 1969.
(22) Hubbard, P. S. *J. Chem. Phys.* **1970**, *53*, 985.
(23) Wennerström, H. *Mol. Phys.* **1972**, *24*, 69.
(24) Bull, T. E.; Forsén, S.; Turner, D. L. *J. Chem. Phys.* **1979**, *70*, 3106.

with one state (bulk water in this case) under "extreme narrowing" conditions show that the longitudinal magnetization decays as a single exponential in all cases of practical interest, while the transverse magnetization, under similar conditions, decays as a sum of three exponentials. However, since the preexponential factors depend on the distribution of nuclei over different sites as well as on the corresponding correlation times[24] the transverse magnetization will also decay exponentially for $P_S \lesssim 0.1$ and $\tau_c \lesssim 50$ ns. In fact, in the experiments reported here the dominating exponential always exceeds 0.99 relative amplitude (except for the most concentrated HPA solutions in Figure 5, where it was 0.95 for R_2 at the highest frequency, and for the highest Lyz and HPA concentrations in Figure 6, where it was 0.8 for R_2 at 13.564 MHz).

For a fast exchange two-state model we may thus write the excess relaxation rates as

$$R_{i,ex} \equiv R_{i,obsd} - R_{ref} = P_{PR}(R_{i,PR} - R_{ref}) \quad (i = 1, 2) \quad (2)$$

where $R_{i,obsd}$ is the observed relaxation rate in a protein solution, R_{ref} is the relaxation rate in pure water of the same temperature, and the mole fraction P_{PR} and relaxation rates $R_{i,PR}$ refer to those water molecules that interact detectably with the protein, i.e., the "hydration water" in the ^{17}O relaxation sense.

Since the experimental data could not be fitted to a simple two-state fast exchange model (two parameters), in which the hydration water is described by a single correlation time, we introduced the three-parameter model described in the following. Protein–water interactions are inherently anisotropic on a time scale that is long compared to the reorientational time of the hydration water.[73] The averaging of the quadrupolar interaction is therefore most conveniently treated as a two-step process.[25,26] In the first step a fast, slightly anisotropic, reorientational motion partially averages the quadrupolar interaction, while in the second step the remaining part of the quadrupolar Hamiltonian is averaged to zero by a slower process, which may consist of protein reorientation, internal motion of protein segments, translational diffusion of water molecules along the protein surface, or water exchange between the hydration region and the bulk. Since no quadrupolar splittings are observed, this slower motion must have a correlation time no longer than the inverse quadrupole coupling constant, i.e., ca. 100 ns.

A detailed analysis[25,26] shows that the quadrupolar Hamiltonian, as well as the correlation functions and spectral densities, can be divided into two terms corresponding to the independent fast and slow motions, respectively. Equation 2 then reads

$$R_{i,ex} = P_{PR}(R_{i,f} + R_{i,s} - R_{ref}) \quad (i = 1, 2) \quad (3)$$

We now assume that there is axial symmetry[70] around the local director (normal to the protein surface) and that the correlation functions are exponential. The latter approximation is reasonable if the local anisotropy of the fast motion is small and if any reorientational motion contributing to the long correlation time is nearly isotropic. An approximation of this kind, although not required for the general conclusions, is convenient for the physical interpretation of the dynamical information. If, furthermore, the fast motion is under "extreme-narrowing" conditions in the investigated frequency range (i.e., if $\tau_f \lesssim 1$ ns), then the two contributions to the excess relaxation rates become[25-29]

$$R_f = (12\pi^2/125)(1 + \eta^2/3 - S^2)\chi^2\tau_f \quad (4a)$$

$$R_{i,s} = (12\pi^2/125)(S\chi)^2 f_i(\tau_s,\omega_0) \quad (i = 1, 2) \quad (4b)$$

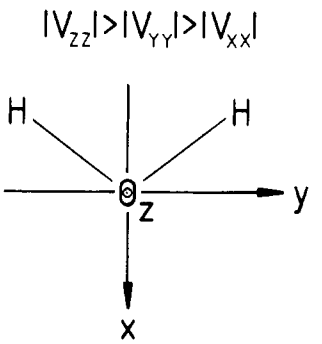

Figure 1. Principal axes system for the electric field gradient tensor at the oxygen nucleus in H_2O.

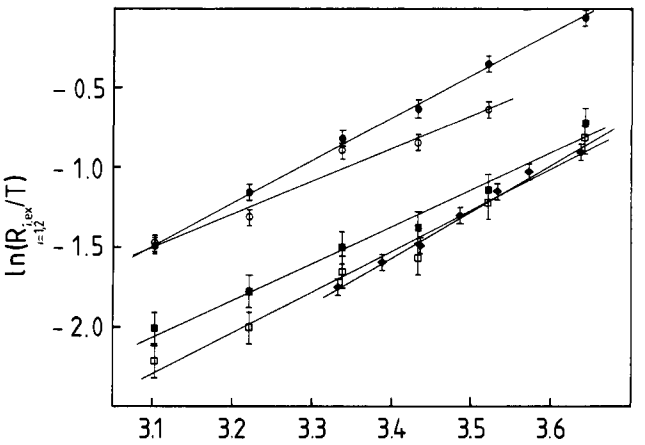

Figure 2. Temperature dependence of the ^{17}O excess longitudinal and transverse relaxation rates for D_2O solutions contaianing oxidized ($R_{2,ex}$ (●), $R_{1,ex}$ (■)) and reduced ($R_{2,ex}$ (○), $R_{1,ex}$ (□)) cyt *c* and HPA ($R_{2,ex}$ (♦). Measurements were made on 5 mM cyt *c* at pD 9.9 and 2.85×10^{-4} M HPA at pD 5.3. Error bars are based on estimated uncertainties in line width measurements (R_2) or standard deviation from inversion recovery semilog plot (R_1).

(R_f, of course, becomes frequency dependent at sufficiently high frequencies). In eq 4 τ_f and τ_s are the correlation times for the fast and slow motions, respectively, and $\chi \equiv |eQV_{zz}/h|$ is the quadrupole coupling constant. The general form of the functions $f_i(\tau_s,\omega_0)$ is not known; they were computed numerically[24] in the process of diagonalization of the total relaxation matrix. The local "order parameter" S is given by[25,30] eq 5, where the S_{ii} are diagonal

$$S = S_{zz} + (\eta/3)(S_{xx} - S_{yy}) = (1/2)[(3\overline{\cos^2\theta} - 1) + \eta\overline{\sin^2\theta\cos 2\phi}] \quad (5)$$

components of the traceless orientation tensor **S** for the water molecule, expressed in the principal axes system of the electric field gradient tensor **V** (Figure 1). The asymmetry parameter for the field gradient is defined as $\eta \equiv (V_{xx} - V_{yy})/V_{zz}$, V_{ii} being components of the electric field gradient at the ^{17}O nucleus expressed in the principal axes system of Figure 1. θ and ϕ are the polar and azimuthal angles, respectively, of the maximal field gradient component V_{zz} with respect to the local director. The averages in eq 5 are to be taken over a time that is long compared to the correlation time τ_f for the fast motion.

Temperature Dependence. To determine whether the fast exchange limit is applicable for the hydration water, i.e., if eq 1 and 2 are valid, we measured relaxation rates as functions of temperature for HPA and cyt *c* (at two pH values). It can be shown under very general conditions that an Eyring plot of $\ln(R_{i,ex}/T)$ vs. $1/T$ yields a line of positive slope in the fast exchange limit.[31]

(25) Wennerström, H.; Lindblom, G.; Lindman, B. *Chem. Scr.* **1974**, *6*, 97.
(26) Berendsen, H. J. C.; Edzes, H. T. *Ann. N.Y. Acad. Sci.* **1973**, *204*, 459.
(27) Wennerström, H., unpublished material.
(28) Abragam, A. "The Principles of Nuclear Magnetism"; Clarendon Press: Oxford, 1961.
(29) Jacobsen, J. P.; Bildsøe, H. K.; Schaumburg, K. *J. Magn. Reson.* **1976**, *23*, 153.
(30) Khetrapal, C. L.; Kunwar, A. C.; Tracey, A. S.; Diehl, P. "Lyotropic Liquid Crystals"; Springer-Verlag: Heidelberg, 1975.
(31) Lindman, B.; Forsén, S. "Chlorine, Bromine and Iodine NMR; Physicochemical and Biological Applications"; Springer-Verlag: Heidelberg, 1976.

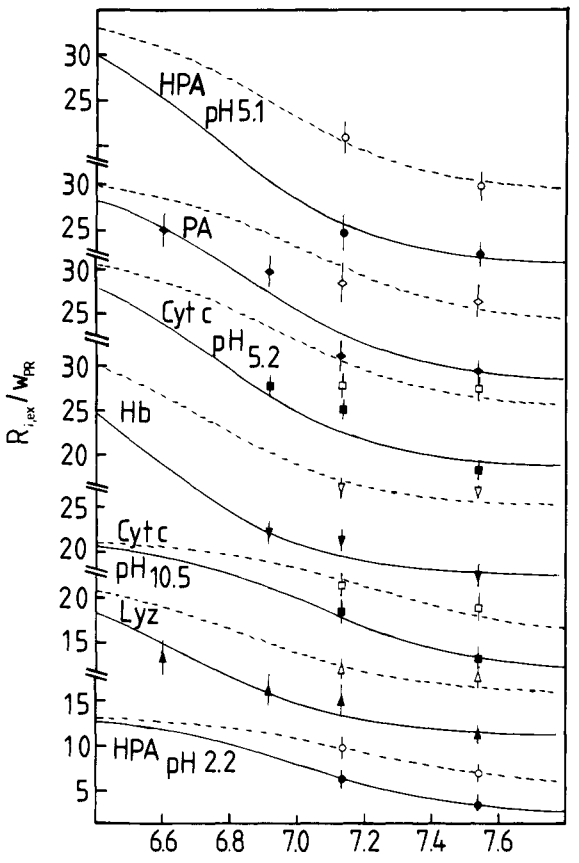

Figure 3. Dispersion of the ^{17}O excess longitudinal (filled symbols, solid curves) and transverse (open symbols, dashed curves) relaxation rates normalized to unit protein concentration w_{PR} (mass %) for aqueous protein solutions at 27.0 °C (28.7 °C for HPA). Concentrations and pH values are listed in Table I. The curves were calculated as explained in the text. Error bars are as in Figure 2.

As seen from Figure 2 this is the case for the investigated protein solutions. (Due to the complicated temperature dependence no simple activation parameter can be extracted from the plot.[32]) According to eq 2 and P_{PR} values from Table I the fast exchange criterion $\tau_{ex} \gg 1/R_{2,PR}$ implies that the average residence time for a water molecule in the hydration region is shorter than ca. 0.1 ms.

Frequency Dependence. Oxygen-17 relaxation rates in aqueous protein solutions are frequency dependent in the range 4–35 MHz, demonstrating that the relaxing motions include a component with correlation time on the order of 10 ns. The "dispersion" of the longitudinal and transverse excess relaxation rates for seven protein solutions is shown in Figure 3. The data were fitted to the model defined by eq 3 and 4 with the three independent parameters $[P_{PR}\chi^2((1 + \eta^2/3 - S^2)\tau_f - \tau_{ref})]$, $[P_{PR}(S\chi)^2$, and τ_s. (Actually, the fit was made with τ_f in eq 4a replaced by f_i (τ_f, ω_0), but it was found that the fast component R_f is under "extreme-narrowing" conditions in the frequency range studied. Thus, it is not possible to separate $[P_{PR}\chi^2(1 + \eta^2/3 - S^2)]$ from τ_f as for the slow component.)

At first glance, the data in Figure 3 may appear insufficient to determine the theoretical curves. However, it should be realized that the two curves are not independent and that a separation of the fast and slow relaxation contributions does not require data from the dispersion region (where $R_{i,ex}$ is frequency dependent), since $R_{2,ex}$ (at all frequencies) contains information about the slow component through the spectral density at zero frequency. From Figure 4, which illustrates the dispersion behavior expected from our model over a larger frequency range in order to include the high- and low-frequency limits of the slow component, one can see that it is sufficient to determine the high-frequency plateau

(32) Stephens, R. S.; Bryant, R. G. *Mol. Cell. Biochem.* **1976**, *13*, 101.

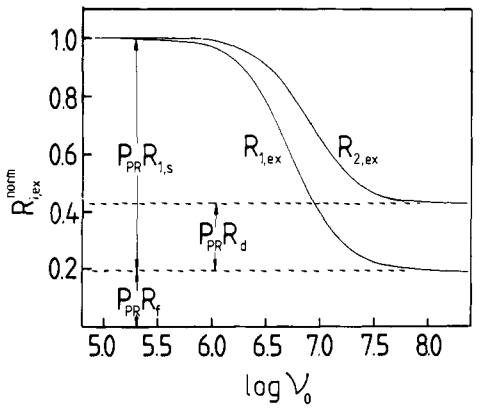

Figure 4. Dispersion of the (normalized) ^{17}O excess relaxation rates showing the limiting behavior and the definition of the slow (low-frequency limit) and fast contributions. In calculating the curves typical values of the three parameters were used.

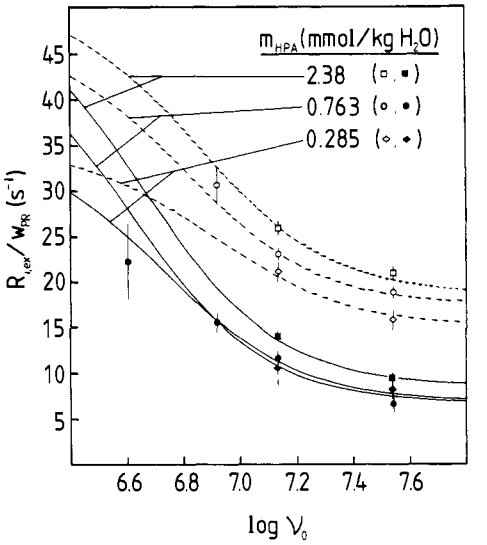

Figure 5. Dispersion of the ^{17}O excess relaxation rates normalized to unit protein concentration w_{PR} (mass %) for aqueous HPA solutions at pH 5.16 ± 0.08. The intermediate concentration was studied at 27.0 °C and the other two at 28.7 °C. The curves (longitudinal, solid; transverse, dashed) were calculated as explained in the text. Error bars are as in Figure 2.

to obtain the two quantities $P_{PR}R_f$ and $P_{PR}R_d$ measuring the fast and slow contributions, respectively.

The dispersion from HPA solutions at three concentrations is shown in Figure 5. The difference in the (normalized) data is partly due to the temperature difference, but effects of protein–protein interaction are also apparent (cf. next section).

The results of fitting the data in Figures 3 and 5 are given in Table I. From the standard deviations of the fits we estimate uncertainties of ca. 20% in the two composite parameters and 10–50% in τ_s (the larger uncertainties here reflect the poor low frequency data). In the limit of exponential relaxtion described by second-rank tensors[28] the ratio $R_d/R_{1,s}$ should equal 0.3. From the fitted parameters we calculated this ratio (Table I) as a test of consistency of the data.

Protein Concentration Dependence. Figure 6 shows the dependence of the ^{17}O transverse relaxation rate on protein concentration for aqueous solutions of lysozyme and human plasma albumin. It is seen that the excess relaxation rate increases linearly up to protein concentrations between 5 and 10%, whereas at still higher concentrations it increases faster than linearly. This behavior is also apparent from Figure 5.

pD Dependence. The pD dependence of the ^{17}O relaxation was studied for D_2O solutions of HPA and IgG; the results are shown in Figure 7. The curves represent the total number of charged residues on the protein. For HPA (Figure 7a), we obtained this

Table I. ^{17}O Relaxation Data for Aqueous Protein Solutions

sample[a]	pH	w_{PR}, mass %	m_{PR}, mmol/kg	$R_2,ex/w_{PR}$ at 13.56 MHz, s^{-1}	$P_{PR}X^{2-}[(1+\eta^2/3-S^2)\tau_f - \tau_{ref}]$, s^{-1}	$10^{-9}\cdot P_{PR}(SX)^2$, s^{-2}	$R_d/R_{1,s}$	$10^2 P_{PR}$	H, g of H_2O/100 g of PR	τ_f, ps	τ_s, ns	$\tau_s/\tau_{rot}^{(2)}$ [b]	mean center-to-center distance in units of diameter of gyration[b]
parvalbumin, pI 4.25	8.99	2.40	2.15	19.5	21.6	4.50	0.31	2.2	88	20	13	4.4	3.8
cytochrome *c*, ferri	5.22	5.00	4.25	17.0	41.1	8.07	0.29	3.9	74	21	16	6.6	3.3
	10.49	5.00	4.25	16.5	36.6	9.37	0.34	4.5	86	17	8		3.3
lysozyme	5.11	8.29	6.31	12.2	44.3	7.89	0.29	3.8	43	23	19	4.6	2.3
hemoglobin, oxy	9.17	4.78	0.779	16.2	34.0	5.47	0.28	2.6	53	25	25	1.9	2.9
plasma albumin[c] (0.15 M KCl)	5.09	1.86	0.285	21.0	13.6	3.34	0.30	1.6	85	17	16	0.4	2.7
	2.18	1.86	0.285	9.9	4.65	2.42	0.34	1.2	62	9	9		2.7
	5.24	4.83	0.763	23.0	33.8	9.74	0.28	4.7	93	15	21		2.0
	5.11	13.7	2.38	25.8	123	31.9	0.25	15	98	16	19		1.4
alcohol dehydrogenase, apo (0.15 M KCl, 25 mM MES)	5.73	3.5	0.46	34.0									2.6
immunoglobulin G, polyclonal (0.15 M KCl, D_2O)	6.0	0.77	0.054	39.0									>3

[a] The medium was H_2O and the temperature 27.0 °C unless otherwise stated. See also Experimental Section. [b] See Table II. [c] All albumin data, except at pH 5.24, refer to 28.7 °C.

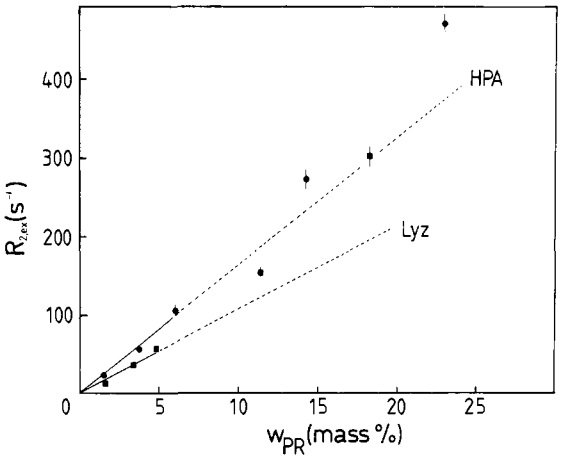

Figure 6. Protein concentration dependence of the ^{17}O excess transverse relaxation rate (at 13.56 MHz) for aqueous solutions of Lyz (pH 5.1) and HPA (pH 5.2) at 28.5 °C. The lines were drawn as an aid to the eye.

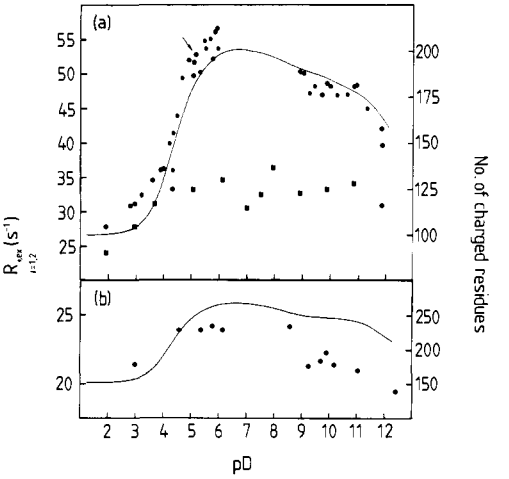

Figure 7. Variation of ^{17}O excess longitudinal (■) and transverse (●, ♦) relaxation rates (13.56 MHz) with pD at 28.0 °C for D_2O solutions containing (a) 2.75×10^{-4} M HPA (0.15 M KCl) and (b) 5.4×10^{-5} M IgG. The data point marked with an arrow was obtained by reverse titration from pD 2. The curves giving the number of charged residues were constructed according to the text.

quantity from a potentiometric titration in 0.15 M KCl/D_2O. The data treatment as well as the number and identity of prototropic groups were the same as in ref 33. The pK_D values so obtained closely agree with previously determined[33] pK_H values corrected for the solvent isotope effect.[34] The curve for IgG (Figure 7b) was calculated from the amino acid composition[35] (assuming that all prototropic residues are accessible for titration) and pK values typically found in proteins[36] corrected for the solvent isotope effect.[34] Figure 7 reveals a correlation between the number of charged residues and ^{17}O relaxation rate, particularly for the carboxylate groups.

Discussion

The Quadrupole Coupling Constant. To separate the quantites P_{PR}, S, and τ_f entering the composite fitted parameters, it is desirable to have an accurate value for the water ^{17}O quadrupole

(33) Halle, B.; Lindman, B. *Biochemistry* **1978**, *17*, 3774.
(34) Laughton, P. M.; Robertson, R. E. In "Solute-Solvent Interactions"; Coetzee, J. F.; Ritchie, C. D., Eds.; Marcel Dekker: New York, London, 1969; Chapter 7.
(35) Edelman, G. M.; Cunningham, B. A.; Gall, W. E.; Gottlieb, P. D.; Rutishauser, U.; Waxdal, M. J. *Proc. Natl. Acad. Sci. U.S.A.* **1969**, *63*, 78.
(36) Steinhardt, J.; Reynolds, J. A. "Multiple Equilibria in Proteins"; Academic Press: New York, 1969; 178.
(37) Schriever, J.; Leyte, J. C. *Chem. Phys.* **1977**, *21*, 265.

coupling constant χ. This quantity may be obtained from the ^{17}O relaxation rate in pure water, which is given by[28] eq 6, provided

$$R = (12\pi^2/125)\chi^2(1 + \eta^2/3)\tau_{rot}^{(2)} \quad (6)$$

that an independent estimate of the second-rank rotational correlation time $\tau_{rot}^{(2)}$ is available. (Here we assume that the ^{17}O quadrupolar relaxation in pure water may be described by a single correlation time.[38])

The standard procedure is to use dielectric relaxation data, from which the first-rank rotational correlation time $\tau_{rot}^{(1)} = 3\tau_{rot}^{(2)}$ may be extracted. To obtain $\tau_{rot}^{(1)}$ from the measured macroscopic dielectric relaxation time τ_{diel}, it is necessary to apply a correction. The exact form of this correction has been a controversial issue, but the most reliable relation is now considered to be[39]

$$\tau_{rot}^{(1)} = \tau_{diel}K^{-1/(2K+1)} \quad (7)$$

where $K \equiv \epsilon_s/\epsilon_\infty$, ϵ_s being the static relative permittivity and ϵ_∞ the same quantity in the high-frequency limit.

From a large number of measurements on different samples using different pulse sequences on several spectrometers, we have determined the ^{17}O relaxation rates $R(H_2O) = 131.0 \pm 2.0$ s^{-1} and $R(D_2O) = 167.4 \pm 2.0$ s^{-1} at 27.0 °C in the absence of exchange broadening. Using $\tau_{diel} = 7.79$ ps, $\epsilon_s = 77.85$, and $\epsilon_\infty = 4.21$ (obtained from a computer fit to dielectric data from seven different studies[40]) for H_2O at 27.0 °C and $\tau_{diel} = 10.03$ ps, $\epsilon_s = 77.23$, and $\epsilon_\infty = 4.0$ for D_2O[41] at 27.0 °C in combination with the above-mentioned ^{17}O relaxation rates, we get from eq 6 and 7: $\chi(1 + \eta^2/3)^{1/2} = 7.58$ MHz for H_2O and 7.56 MHz for D_2O. The excellent agreement is consistent with the similar electron distribution and hydrogen (deuteron) bond geometry in H_2O and D_2O. Based on the estimated uncertainties in the ^{17}O relaxation rates, a 1% uncertainty in τ_{diel}, and a 5% uncertainty in the internal field correction, we get an uncertainty of ±0.20 in the effective quadrupole coupling constant. The asymmetry parameter is assumed to be the same as in ice, i.e., $\eta = 0.93$ for both H_2O[78] and D_2O.[42] With this value, we finally arrive at the best estimate for the ^{17}O quadrupole coupling constant in H_2O (D_2O) of 6.67 ± 0.20 MHz, virtually the same as the experimental value[42] for D_2O ice (6.66 ± 0.10 MHz). Previous estimates of χ for liquid water (see for example ref 38) are higher by 15–25%, mainly due to the use of the questionable[39] internal field correction factor $(2\epsilon_s + \epsilon_\infty)/(3\epsilon_s)$. (It has been shown[43] that χ is temperature independent in the range 5–95 °C, so our conclusions from the temperature dependence of the ^{17}O relaxation rate in protein solutions are not invalidated for this reason.)

In using the χ value determined for pure water in eq 4, we have neglected any influenced from the charged protein surface on the ^{17}O quadrupole coupling constant. To examine the validity of this assumption, we performed ab initio calculations on the system $Li^+(H_2O)$.[44] The components of the electric field gradient tensor at the oxygen nucleus were computed for variable oxygen–lithium distances, and different orientations. As expected, the largest effects were observed when the ion approached along a line bisecting the lone pairs of the water molecule (the $-x$ direction in Figure 1). The results for this case are shown in Figure 8. At the computed O–Li^+ equilibrium distance of 0.185 nm, χ is reduced by ca. 6%, while at a typical oxygen-charged residue distance of 0.32 nm the reduction is merely 2.5%. The asymmetry parameter passes through a minimum, and at 0.32 nm it is reduced by less than 10%. These results thus justify the approximation of an unaltered quadrupole interaction for the hydration water as compared to bulk water.

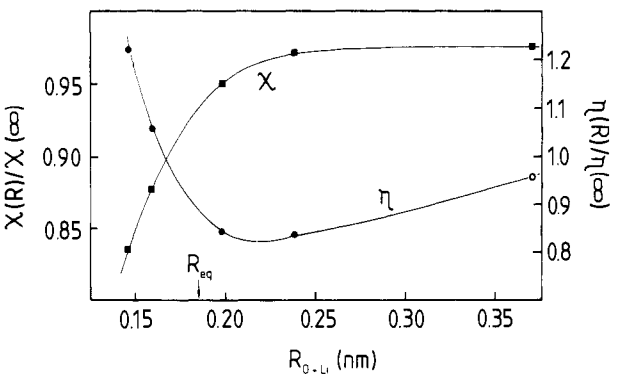

Figure 8. The water ^{17}O quadrupole coupling constant χ and asymmetry parameter η as functions of the distance to a lithium ion approaching along a line bisecting the water lone pairs. The data points were calculated as explained in ref 44.

The Order Parameter. The fitted parameters $[P_{PR}(S\chi)^2]$ could now be used to obtain order parameters S with P_{PR} values calculated from the extent of hydration as determined by some other method. Now, hydration water is usually defined as the water molecules whose properties differ measurably from those of bulk water.[1] To the extent that different experimental techniques probe different interactions and are influenced differently by the dynamics in the system, this must be considered an operational definition. Thus, we will not choose this line of analysis, but rather try to estimate the order parameter, which should vary little with the nature of the protein, and then calculate the extent of hydration (from P_{PR}) for different proteins.

In a system which is anisotropic on a time scale of the order of $1/\chi$, the ^{17}O spectrum will be split into five equidistant peaks with intensity ratios[28] of 5:8:9:8:5 and frequency separation[25]

$$\Delta = (3/40)P|S|\chi \quad (8)$$

where P is the mole fraction of hydration water and the other quantities have been defined above. This equation is valid for a powder sample (no macroscopic alignment), assuming a fast exchange two-state model (hydration water and bulk water).

We chose to study the familiar water–sodium octanoate–decanol system[45] which forms lyotropic liquid crystals with surface charge densities similar to those in globular proteins. At 27 °C we obtained for the product $P|S|$ 9.40×10^{-3} for the hexagonal E phase (90.5, 9.5, 0 mol %) and 5.91×10^{-3} for the lamellar D phase (94.3, 1.5, 4.2). To get an estimate for P, we assume that

(38) Hindman, J. C.; Zielen, A. J.; Svirmickas, A.; Wood, M. *J. Chem. Phys.* **1971**, *54*, 621.
(39) Böttcher, C. J. F.; Bordewijk, P. "Theory of Electric Polarization", 2nd ed., Elsevier: Amsterdam, 1978; Vol. II, Chapter X.
(40) Hasted, J. B. In "Water-A Comprehensive Treatise"; Franks, F., Ed; Plenum Press: New York, 1972; Vol. 1, Chapter 7.
(41) Grant, E. H.; Shack, R. *J. Chem. Soc., Faraday Trans. 1* **1969**, *65*, 1519.
(42) Spiess, H. W.; Garett, B. B.; Sheline, R. K.; Rabideau, S. W. *J. Chem. Phys.* **1969**, *51*, 1201.
(43) Garett, B. B.; Denison, A. B.; Rabideau, S. W. *J. Phys. Chem.* **1967**, *71*, 2606.
(44) Engström, S. unpublished results. The calculations were done with the program "MOLECULE" (Almlöf, J. USIP Report 72-09, University of Stockholm, 1972; USIP Report 74-09, University of Stockholm, 1974), using a H_2O basis set from: Clementi, E.; Popkie, H. *J. Chem. Phys.* **1972**, *57*, 1077. For the isolated H_2O molecule this basis set yielded $V_{zz} = 1.8827$, $V_{yy} = -1.6631$, $V_{xx} = -0.2196$ (atomic units), and $\eta = 0.800$ in close agreement with previous calculations (see, for example: Neumann, D.; Moskowitz, J. W. *J. Chem. Phys.* **1968**, *49*, 2056; Harrison, J. F. *Ibid.* **1967**, *47*, 2990).
(45) Mandell, L.; Fontell, K.; Ekwall, P. *Adv. Chem. Ser.* **1967**, *No. 63*, 89.
(46) Moews, P. C.; Kretzinger, R. H. *J. Mol. Biol.* **1975**, *91*, 201.
(47) Margoliash, E.; Fitch, W. M.; Dickerson, R. E. *Brockhaven Symp. Biol.* **1968**, *No. 21*, 259.
(48) Chipman, D. M.; Sharon, N. *Science (Washington, D.C.)* **1969**, *165*, 454.
(49) Dickerson, R. E. In "The Proteins", 2nd ed.; Neurath, H.; Ed.; Academic Press: New York, 1964; Vol. II.
(50) Scheider, W.; Dintzis, H. M.; Oncley, J. L. *Biophys. J.* **1976**, *16*, 417 (corrected for hydration water).
(51) Eklund, H.; Nordström, B.; Zeppezauer, E.; Söderlund, G.; Ohlsson, I.; Boiwe, T.; Söderberg, B.-O.; Tapia, O.; Brändén, C.-I.; Åkeson, Å. *J. Mol. Biol.* **1976**, *102*, 27.
(52) Squire, P. G.; Himmel, M. E. *Arch. Biochem. Biophys.* **1979**, *196*, 165.
(53) Ise, N.; Okubo, T.; Hiragi, Y.; Kawai, H.; Hashimoto, T.; Fujimura, M.; Nakajima, A.; Hayashi, H. *J. Am. Chem. Soc.* **1979**, *101*, 5836.

the hydration numbers are 2–6 for the carboxylate and 1–3 for the hydroxyl groups. This yields $|S|$ values of 0.015–0.045 for the E phase and 0.026–0.077 for the D phase. Considering the similarity of the aggregate surfaces in these mesophases with the protein surface, it is reasonable to assume that the local anisotropy of the hydration water is roughly the same in both types of system. Since we are interested in the local order parameter, the value for the hexagonal phase should be multiplied by 2 (the translational diffusion around the hexagonal aggregates reduces the quadrupole interaction by a factor of 2 as compared to that of the lamellar phase[25]). Thus, we arrive at an estimate of $|S| = 0.06 \pm 0.03$ for the hydration water of proteins.

Extent and Nature of Hydration. Using $\chi = 6.67$ MHz and $|S| = 0.06$ (cf. preceding sections) for all protein solutions together with protein concentrations (Table I) and molar masses (Table II), we calculated the extent of hydration H (grams of hydration water per 100 g of dry protein) from the fitted parameters $[P_{PR}(S\chi)^2]$. The resulting H values (Table I) correspond to approximately two molecular layers (cf. monolayer hydration in Table II) for all proteins studied except lysozyme, where the ^{17}O hydration is only slightly more than a monolayer.

When the protein concentration is increased, effects in both P_{PR} and $R_{i,PR}$ are expected. At low protein concentrations P_{PR} (and H) should increase linearly with increasing protein concentration, whereas a slower increase is expected at higher concentrations because of overlap between hydration regions. On the other hand, τ_s increases (resulting in an increased $R_{i,PR}$) with increasing protein concentration because of electrostatic repulsion between the protein molecules (see the section on dynamics of hydration). From Figure 6 it is seen that this dynamic effect dominates. The same behavior has been observed in water ^1H relaxation measurements on bovine serum alubumin solutions.[9]

The reported magnitudes of hydration, being operationally defined and imprecise due to uncertainty in the order parameter, are of lesser interest than the variation in H with the nature of the protein. With the assumption that S varies less among different proteins than between protein and liquid crystal, the relative variations in H should be more accurate (about 20% uncertainty) than the absolute values. From Tables I and II it is seen that no correlation exists between the ^{17}O hydration and "geometrical hydration" (area/volume ratio and monolayer) or hydrodynamic hydration. Clearly, more subtle effects dominate the variation in protein hydration. A clue to the nature of these effects is provided by the pD dependence of the ^{17}O relaxation rates (Figure 7), which reveals that charged residues, particularly carboxylate, are more extensively hydrated than uncharged residues. This finding is in agreement with low-temperature proton NMR work[1,11] on proteins and polypeptides, giving hydration numbers of 6–7.5 for anionic, 3–4.5 for cationic, 2–3 for polar uncharged, and 1 for apolar residues.

In Figure 9a the ^{17}O extent of hydration H is plotted vs. the "percentage" of charged residues (Table II) with the anionic residues weighted twice as much as the cationic ones in accord with the results of Kuntz and co-workers. The linear correlation for the "nearly neutral" (pH 5–9) protein solutions is striking, considering that individual proteins should vary in the extent of exposure of charged residues (cf. for example, the proposed "salt bridges" between subunits in HPA[54]). The hydration of HPA at low pH and of cyt c at high pH deviates considerably from the general trend in Figure 9a. This is most likely due to an increased fraction of exposed uncharged polar and apolar residues at these extreme pH values (cf. the acid expansion of HPA[55,56]), which should result in a larger intercept.

If the fast correlation time τ_f is independent of the nature of the protein, then the quality $P_{PR}R_f/w_{PR}$, obtained from the fit to the dispersion data, should be proportional to H. As seen from Figure 9b, the trend is much the same: the larger scatter indicates

Table II. Physicochemical Data for Proteins

protein (source)	molar mass,[a] kg/mol	no. of subunits	exptl pH	molecular dimens,[c] nm (ref)	axial ratio[d]	R_G,[e] nm	$\tau_{rot}^{(2)}$,[f] ns	area/vol ratio,[g] nm^{-1}	percent of residues[h]				estimates of hydration, g of H_2O/100 g of protein	
									anionic	cationic	polar neutral	apolar	monolayer[i]	hydrodynamic[k]
parvalbumin, pI 4.25 (carp muscle)	11.50	1	8.99	3.0 × 3.0 × 3.6 (46)	1.2	1.2	2.9	1.9	19.1	12.3	24.1	44.5	41.9	
cytochrome c, ferri (horse heart)	12.38	1	5.22 10.49	2.5 × 2.5 × 3.7 (47)	1.5	1.1	2.4	2.2	10.8 11.9	22.8 12.8	35.8 44.8	30.5 30.5	31.2	24
lysozyme (hen egg white)	14.32	1	5.11	3.0 × 3.0 × 4.5 (48)	1.5	1.4	4.2	1.8	7.6	14.5	43.6	34.4	39.9	57
hemoglobin, oxy (human)	64.37	4	9.17	5.0 × 5.5 × 6.4 (49)	1.2	2.2	13	1.1	11.5	9.2	31.9	47.4	23.6	74[l]
plasma albumin (human)	66.50	3[b]	5.09 2.18	3.5 × 3.5 × 14.0 (50)	4.0	3.3	40	1.4	15.6 0.3	17.0 17.1	27.4 42.7	50.2 39.9	28.0	35
alcohol dehydrogenase, apo (horse liver)	79.87	2	5.73	4.5 × 6.0 × 11.0 (51)	2.1	3.0	31	1.0	10.2	13.1	33.1	43.6	28.9	37
immunoglobulin G, polyclonal (human)	150.0	3[b]	6.0						5.5	11.3	46.3	36.9		

[a] From amino acid composition. [b] Covalently linked. [c] From X-ray crystallography, i.e., excluding hydration water. [d] For prolate ellipsoid: $2a \times 2a \times 2c$, $n = c/a$. [e] Radius of gyration for prolate, $R_G = c[(2/n^2 + 1)/5]^{1/2}$. [f] For a sphere of radius $R = R_G + 0.3$ nm, obeying the Debye-Stoke-Einstein relation $\tau_{rot}^{(2)} = 4\pi\eta R^3/(3kT)$, where $T = 300$ K and $\eta = 8.50 \times 10^{-4}$ kg ms^{-1}. [g] For prolate: $A/V = (3/2c)[1 + (n/x)\arcsin x]$, where $x = (1 - 1/n^2)^{1/2}$. [h] At experimental pH, assuming all residues available for titration with pK values from ref 36 or ref 33 (HPA). [i] For prolate and 0.12 nm^2 surface area per H_2O molecule. [k] From sedimentation and diffusion coefficients.[52] [l] Horse hemoglobin.

(54) Vijai, K. K.; Foster, J. F. *Biochemistry* **1967**, *6*, 1152.
(55) Sogami, M.; Foster, J. F. *Biochemistry*, **1968**, *7*, 2172.
(56) Peters, T., Jr., In "The Plasma Proteins", 2nd ed.; Putnam, F. W.; Ed.; Academic Press: New York, 1975; Vol. I.

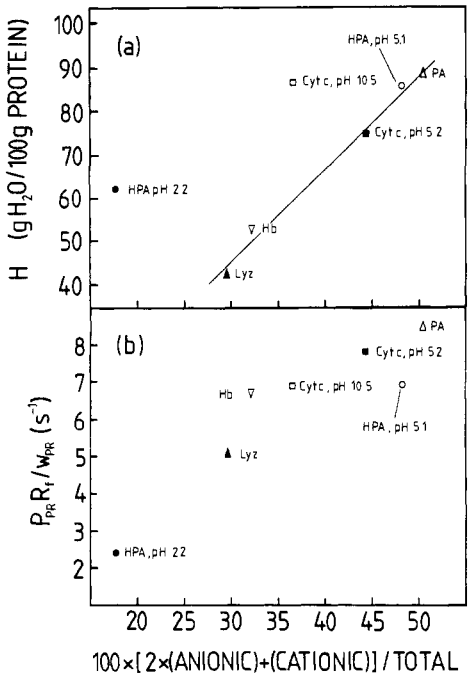

Figure 9. (a) The extent of hydration (from ^{17}O relaxation) vs. "percentage" (weighted) of charged residues. The line is a least-squares fit to the five data points in the pH range 5–9 (see Table I). (b) The normalized fast contribution to the ^{17}O excess relaxation rate vs. "percentage" (weighted) of charged residues.

a small variation in τ_f with the nature of the protein (cf. next section). Note that the correlation evident from Figure 9b is independent of any assumptions about the order parameter (as long as $S^2 \ll 1$).

The water–HPA interaction in the acidic pH range deserves special consideration. From Figures 7a and 9 it is clear that an appreciable reduction in hydration occurs as pH (pD) is lowered from 5 to 2. The decrease in excess ^{17}O relaxation rates in Figure 7a is, however, partly due to a variation in the slow correlation time τ_s. This follows from the much larger effect on $R_{2,ex}$ as compared to $R_{1,ex}$ and accordingly the fitted τ_s decreases from 16 ns at pH 5.1 to 9 ns at pH 2.2 (Table I). (A reduced correlation time for the expanded HPA molecule was also deduced from ^{35}Cl magnetic relaxation studies[33] and is explained by independent reorientation of the subunits.) The decrease in H between pH 5.1 and 2.2 is 27% (Figure 9a), in good agreement with the low-temperature proton NMR results[11] of 24%. Other measurements have, however, been interpreted as an increased hydration upon lowering of pH from 5 to 2, by 67% according to measurements of the $H_2{}^{18}O$ self-diffusion coefficient[57] and by 50% according to dielectric relaxation studies.[58] Without going into a detailed discussion of the theoretical basis of the data reduction in these techniques, we want to point out the possibility that these results are influenced by the greatly increased size and anisotropy of the albumin molecule which occurs during the N–F transition around pH 4.2 and the acid expansion in the pH range 2–4.[55,56]

Dynamics of Hydration. The fast correlation time τ_f for the local, slightly anisotropic water reorientation was calculated from the ratio of the two composite parameters by using an order parameter $|S| = 0.06$ (cf. above). As expected τ_f is, within the estimated uncertainty (ca. 30% not counting the uncertainty in S, otherwise of the order 100%), the same for all protein solutions (except possibly HPA at pH 2.2) with an average of 20 ps (Table I). Thus the hydration water is, on the average, hindered in its reorientational motion by a factor of ca. 8 relative to bulk water ($\tau_{rot}^{(2)} = 2.40$ ps for pure H_2O at 27.0 °C according to the dielectric data cited above). This is of the same order of magnitude as the slowing down of the hydration water reorientation in aqueous electrolyte solutions found by NMR relaxation[60] (e.g., a factor of 1.5–3.5 for CO_3^{2-}, CCl_3COO^-, Li^+, and Na^+). On the other hand, a large amount of dielectric[1,74] and magnetic[9,75] relaxation data from aqueous protein solutions have been interpreted in terms of hydration water correlation times in the nanosecond (or even microsecond[72]) range. Such slow reorientational rates are clearly inconsistent with our data.

The shorter τ_f of 9 ps found for HPA at pH 2.2 (Table I) is explained by the fact that virtually all the ca. 105 carboxylate groups, which otherwise make a major contribution to the slowing down of water reorientation, are protonated at this pH.

The slow correlation time τ_s (Table I), obtained directly from the fit to the dispersion data, is in all cases (except for HPA) significantly longer than the rotational correlation time $\tau_{rot}^{(2)}$ calculated from the Debye–Stokes–Einstein equation with the radius of gyration corrected for hydration (Tables I and II). Similarly long correlation times have been observed by other methods, e.g., proton and deuteron NMR dispersion,[4,6] ^{13}C relaxation,[61] light scattering,[62] and dielectric relaxation.[63,64] As an explanation we suggest that electrostatic repulsion between the densely spaced (cf. mean center-to-center distance in Table I) and highly charged protein moleucles has an ordering effect on the system. This hypothesis is supported by the fact that concentrated solutions of micelles[65] and polyelectrolytes[53] yield X-ray diffraction patterns and thus are lattice-like. If this long-range Coulombic protein–protein interaction is important, one would expect a decreased τ_s with increasing salt concentration. This is indeed found; only for HPA was the ^{17}O dispersion measured in the presence of added electrolyte (0.15 M KCl) and here τ_s is smaller than the calculated $\tau_{rot}^{(2)}$. The hypothesis also predicts that τ_s should increased with increasing protein concentration; that this is the case can be seen from the HPA data in Table I (note that τ_s for the intermediate concentration refers to a slightly lower temperature) and from the protein concentration dependence for Lyz and HPA (see above). The variation in the ratio $\tau_s/\tau_{rot}^{(2)}$ (Table I) is probably due to structural differences; the ordering effect should increase with increasing molecular anisotropy.

Concluding Discussion

We now recapitulate the arguments that led us to formulate the model defined by eq 3 and 4 and then summarize the main results from our ^{17}O relaxation data analyzed in terms of this model. First it is quite clear (cf. Figures 3–5) that the dispersion of the excess relaxation rates cannot be described by a single correlation time, i.e., by a simple two-state fast exchange model, rather a two-correlation time model is needed. Now, the two correlation times for the hydration water may be interpreted in two ways.

The first model, which, with various modifications, has been used in most protein hydration NMR dispersion work (see, for example, ref 4, 6–10), consists of two physically distinct classes of hydration water. Such a model is unsatisfactory for two reasons. (i) It is unlikely that two classes of hydration water, both in the fast exchange limit, should have reorientation times differing by 3 orders of magnitude. (ii) If the long correlation time is associated with rigidly bound water molecules, then unreasonable low degrees of hydration result; putting $S = 1$ in eq 4b reduces all H values by a factor of 3.6×10^{-3}; e.g., for lysozyme this leads to the absurd situation that the slow contribution to the relaxation rate is due

(57) Sandeaux, J.; Kamenka, N.; Brun, B. *J. Chim. Phys.* **1978**, *75*, 895.
(58) Kashpur, V. A.; Maleev, V. Ya; Shchegoleva, T. Yu. *Stud. Biophys.* **1975**, *48*, 97.
(59) Einarsson, R., personal communication.
(60) Hertz, H. G. In "Water-A Comprehensive Treatise"; Franks, F., Ed.; Plenum Press: New York, 1973; Vol. 3, Chapter 7.
(61) Wilbur, D. J.; Norton, R. S.; Clouse, A. O.; Addleman, R.; Allerhand, A. *J. Am. Chem. Soc.* **1976**, *98*, 8250.
(62) Dubin, S. B.; Clark, N. A.; Benedek, G. B. *J. Chem. Phys.* **1971**, *54*, 5158.
(63) Grant, E H.; South, G. P.; Takashima, S.; Ichimura, H. *Biochem. J.* **1971**, *122*, 691.
(64) Schlecht, P.; Mayer, A.; Hettner, G.; Vogel, H. *Biopolymers* **1969**, *7*, 963.
(65) Hartley, G. S. In "Micellization, Solubilization and Microemulsions"; Mittal, K. L.; Ed.; Plenum Press: New York, 1973; Vol. 1, p 23.

to 1.2 water molecules (cf. ref 4 and 6).

In the other type of two-correlation time model there is only one class of hydration water, i.e., this is a two-state model. Due to the influence of the protein surface, the reorientation of the hydration water is anisotropic; hence it must be described by two correlation times. This model is consistent with the magnitude of the two correlation times τ_f and τ_s and is also physically attractive in view of the similarity of the local environment near a protein surface and that in anisotropic lyotropic liquid crystals. Similar models have been used to interpret nuclear magnetic relaxation data in solutions of micelles[25] and biological macromolecules.[66,73] Recently a qualitative reinterpretation of previous[4,6] proton and deuteron dispersion data for protein solutions using this model has been published.[67] In that work, however, the contribution from the fast motion (eq 4a) was neglected.

The emerging picture of protein hydration is intermediate between the two extremes of polarized multilayers[68] on the one hand and a small number of irrotationally bound water molecules[4,6] on the other. Approximately two layers of water are, on the average, hindered in their reorientation by a factor of ca. 8. This rapid local motion has a small anisotropic component which is averaged out by protein reorientation. Charged residues, particularly carboxylate, are more extensively hydrated than other residues. This fact accounts for the variation in the extent of hydration between different proteins (Figure 9a).

Note **Added in Proof**: Since the completion of this work, it has been shown[79] that existing analytical expressions[80] for the relaxation rates, i.e., for the functions $f_i(\tau_s,\omega_0)$ in eq 4b, are accurate to better than 2% for the present data. The numerical diagonalizations of the relaxation matrices that were performed in this work, although correct, are thus unneccessary. Furthermore, a detailed derivation and discussion of the "two-step averaging" relaxation model (eq 3-5) will appear shortly (Wennerström, H.; Halle, B. *J. Chem. Phys.*, submitted).

Acknowledgment. We wish to thank Maj-Lis Fontell for carrying out the potentiometric titration, Lennart Nilsson for spectrometer innovations and maintenance at all hours, Roland Einarsson for generous supplies of HPA, and Håkan Wennerström for numerous enlightening discussions on relaxation theory. We are also grateful to Marianne Swärd for preparing the parvalbumin and to Inger Andersson for preparing the ADH. The project was supported by a grant from the Swedish Natural Sciences Research Council. B.H. also wishes to acknowledge a grant from Stiftelsen Bengt Lundvists Minne.

(66) Forsén, S.; Lindman, B. *Methods Biochem. Anal.* **1980**, *26*.
(67) Walmsley, R. H.; Shporer, M. *J. Chem. Phys.* **1978**, *68*, 2584.
(68) Ling, G. N. *Biophys. J.* **1973**, *13*, 807.
(69) Meiboom, S. *J. Chem. Phys.* **1961**, *34*, 375.
(70) In fact, it can be shown that only threefold symmetry is required.
(71) Koenig, S. H.; Bryant, R. G.; Hallenga, K.; Jacob, G. S. *Biochemistry* **1978**, *17*, 4348 and references therein.
(72) Fung, B. M. *Biophys. J.* **1977**, *18*, 235.
(73) Packer, K. J. *Philos. Trans. R. Soc. London, Ser. B* **1977**, *278*, 59.
(74) Grant, E. H.; Sheppard, R. J.; South, G. P. "Dielectric Behaviour of Biological Molecules in Solution"; Clarendon Press: Oxford, 1978.
(75) Fung, B. M.; McGaughy, T. W. *Biophys. J.* **1979**, *28*, 293.
(76) Meirovitch, E.; Kalb, A. J. *Biochim. Biophys. Acta* **1973**, *303*, 258.
(77) Rose, K. D.; Bryant, R. G. *J. Am. Chem. Soc.* **1980**, *102*, 21.
(78) Edmonds, D. T.; Zussman, A. *Phys. Lett.* **1972**, *41A*, 167.
(79) Halle, B.; Wennerström, H. *J. Magn. Reson.* **1981**, in press.
(80) McLachlan, A. D. *Proc. R. Soc. London, Ser. A* **1964**, *280A*, 271.

Gas-Phase Ion Chemistry of $TiCl_4$ and CH_3TiCl_3. Reaction of $CH_3TiCl_2^+$ with Ethylene

Jack S. Uppal, Douglas E. Johnson, and Ralph H. Staley*

Contribution from the Department of Chemistry, Massachusetts Institute of Technology, Cambridge, Massachusetts 02139. *Received July 11, 1980*

Abstract: $TiCl_4^+$ and $TiCl_3^+$ are the principal ions produced by electron-impact ionization of $TiCl_4$. Both react with $TiCl_4$ to give $Ti_2Cl_7^+$. Reactions of this and other species of the form $TiCl_3(ligand)^+$ allow the determination of an order of relative ligand binding energies to $TiCl_3^+$ of MeF < $TiCl_4$ < MeCl < EtCl < benzene. MeI, propylene, and butenes are also found to be stronger ligands for $TiCl_3^+$ than $TiCl_4$. Study of halide-transfer and proton-transfer reactions leads to determination of the thermochemical results: $D(TiCl_3^+-Cl^-) = 217 \pm 11$ kcal/mol, $D(TiCl_3^+-F^-) = 254 \pm 4$ kcal/mol, and $PA(TiCl_4) \equiv D(TiCl_4-H^+) = 175 \pm 11$ kcal/mol. Chloride transfer from CH_3TiCl_3 to $TiCl_3^+$ yields $CH_3TiCl_2^+$ as the major ion at intermediate times in the ion chemistry of CH_3TiCl_3. $CH_3TiCl_2^+$ reacts with C_2H_4 to give $C_3H_5TiCl_2^+$ with H_2 elimination. $C_3H_5TiCl_2^+$ does not react further with ethylene. With C_2D_4, HD elimination predominates (>85%). A mechanism involving insertion of C_2D_4 into the Ti,C bond in $CH_3TiCl_2^+$ followed by 1,2-elimination of HD at the β- and γ-carbons is inferred. This demonstrates carbon–carbon bond formation and chain growth in a Ziegler–Natta catalyst site model system, but this gas-phase bimolecular process does not lead to continued polymerization because disposal of the excess internal energy of the complex results in chain termination by unimolecular decomposition.

The active sites of certain Ziegler–Natta catalysts for the polymerization of ethylene are thought to involve a Ti(IV) species which likely has at least a partial positive charge.[1] In particular, the active catalyst system CH_3TiCl_3·CH_3AlCl_2 appears to involve the $[CH_3TiCl_2]^+[CH_3AlCl_3]^-$ ion pair which may be partly or wholly dissociated.[2] Studies of the gas-phase ion chemistry of Ti(IV) species can thus be expected to provide useful mechanistic and thermochemical data leading to improved understanding of the chemistry of the Ziegler–Natta class of catalysts.

Ridge has investigated the initial reactions of ions derived from electron-impact ionization of $TiCl_4$ with a variety of organic molecules using ion cyclotron resonance (ICR) drift techniques.[3-5] In this paper we report the results of studies using ICR trapping

(1) Boor, J., Jr. "Ziegler-Natta Catalysts and Polymerizations"; Academic Press: New York, 1979.
(2) Bestian, H.; Clauss, K. *Angew. Chem., Int. Ed. Engl.* **1963**, *2*, 704.
(3) Allison, J.; Ridge, D. P. *J. Am. Chem. Soc.* **1977**, *99*, 35-39.
(4) Allison, J.; Ridge, D. P. *J. Am. Chem. Soc.* **1978**, *100*, 163-169.
(5) Kinser, R.; Allison, J.; Dietz, T. G.; de Angelis, M.; Ridge, D. P. *J. Am. Chem. Soc.* **1978**, *100*, 2706-2708.

0002-7863/81/1503-508$01.00/0